International Journal of Scientific Research in Physics and Applied Sciences
Vol.6, Issue.2, pp.43-51 April (2018)

Research Paper

E-ISSN: 2348-3423

Synthesis Growth, structural, optical, SHG and characterization a new organic potential novel material Z-scan studies third order nonlinear optical material on single crystal of N-(tert-butyl)-2-(2-nitrophenyl) imidazo [1,2-a]Pyridin-3-amines

K.Elumalai Kuppan[1]*, K.Sakthiumurugesan[2]

[1]Department of physics, presidency college (Autonomous),Chennai, India
[2]Department of physics, presidency college (Autonomous),Chennai, India

Corresponding author: elumalai9176@gmail.com

Available online at: www.isroset.org

Received 20/Dec/2017, Revised 14/Jan/2018, Accepted 25/Feb/2018, Online 30/Apr/2018

Abstract- In this work, an organic crystal, Synthesis of N-(tert-butyl)-2(2-nitrophenyl[1,2-a]Pyridin-3-amine, pdno2 single crystal were grown by slow evaporation solution growth method and the properties of the grown crystals were investigated . The formation of salt has been confirmed by single crystal X-ray diffraction and NMR Spectroscopic technique. The crystal structure was determined by single crystal x-ray diffraction analysis and it belongs to monoclinic system with the space group c1 Fourier transform infrared spectral study has been carried out to confirm the presence of various functional groups, UV-Vis-NIR study showed that the pdno2 crystal has a wide transmission window with low near-UV cut off wavelength at 231nm.The UV-Vis-NIR transmission spectrum recorded to find the optical transmittance window and lower cut off wavelength of the salt crystal. Raman spectra correlate very well with the structural data and illustrated the sub title choice of the ligands used can affect the vibrational characteristics of the Mo-o bonds vibration modes were assigned using FT-IR and FT-Raman spectra. Mass spectroscopy transmittance studies revealed that the pdn02 crystal has a wide transmission range from 250to900 nm with the lower cut 0f wavelength of 150nm. Thermal properties were investigated using TGA/DSC analyses .The thermal stability of the compound was investigated by carrying out TGA/DSC analyses simultaneously .The second harmonic generation in the crystal was confirmed by the modified Kurtz-perry powder test employing the Nd: YAG laser as the source for infrared radiation. Third order nonlinear optical properties nonlinear absorption coefficient, nonlinear refractive index and third order nonlinear susceptibility was calculated by Z-scan method using 632.8nm He-Ne laser.

Keywords- crystal structure ,FTIR, Differential Scanning Calorimeter, Thermo gravimetric Analyses, NMR, Second Harmonic Generation, Third harmonic Generation, Raman Spectroscopy. UV-Vis –NIR Spectrum, Mass spectroscopy,

I. INTRODUCTION

Organic material systems have been extensively attracting candidate used in the synthesis of efficient second and TONLO materials due to its quick NLO response with the enhanced figure of merit. In this organic ionic crystals have lead high resolution because of its electro delocalization behaviors inherent facile flexibility second harmonic generation efficiency with large LDT s value wide optical transparency high . pdno2 is an important inorganic NLO crystal and it is successfully used for frequency conversion of laser radiation to the mass spectroscopy region. The application of NLO crystals is required in all frequency ranges but their demand in producing laser beams in UV visible regions is growing enormously pzno2 crystals are reliable materials for effective nonlinear process. Thermal stability FT-IR and FT-Raman mechanical thermal ,SGH and third order nonlinear optical properties of pdno2 crystals .SGH materials are much warranted because of their potential application in the field materials was synthesized and the single crystals were grown and characterized through electronic , vibrational, absorptions, nuclear, magnetic resonance spectral studies and TGA/DSC and nonlinear optical studies. In this paper for the first time we report the synthesis ,growth, structural and physical properties of the title crystal pyridine-3-amine.s

II. EXPERIMENTAL PROCEDURE

synthesis of N-(tert-butyl)-2-(2-nitrophenyl)imidazol[1,2-a]pyridine-3-aamine:pdno2 2-Nitro benzaldehyde (1mmol),2-Amino pyridine (1mmol0,tertiary Butyl isocyanide (1mmol) and ethanol (8ml) were added to 50ml RB flask .The reaction mixture was stirred at room temperature with catalytic amount of Iodine for about 24 hours. An orange –yellowish precipitate was formed .check TLC in hexane: ethyl acetate (65:35) percentage used as eluting solvents. The precipitate was filtered off, washed

with excess ethanol and dried under vacuum. Finally collected the precipitated and crystallized from ethanol to get 98% yield and check the further spectrum data analysis.

Single crystal X-ray diffraction analysis

Single crystal of the compound suitable for X-ray diffraction was obtained by slow evaporation method . Three dimension intensity data were collected on a BRUKER8 SMART APEX CCD Diffractometer Using graphite Monochromatized MO-KX radiation (x=0.71073 A) at Department of chemistry, IIT, Chennai, India. The structure was solved by direct methods and refined on F2 by full-matrix least-squares procedures using the SHELXL programs9.All the non-hydrogen atoms were refined using isotropic and later anisotropic thermal parameters.The hydrogen atoms were included in the structure factor calculation at idealized positions by using a riding model, but not refined .Image were created with ORTEP-3.The crystallographic data for the compound are listed in table 1.The title crystal belongs to monoclinic crystallographic system with non-centrosymmetry space group.c1c1 .The unit cell parameters are a=16.0877(10)A, b=22.0452(13)A ,c=17.8670(11) A,And volume V=6326.7(7)A. The intermolecular N-H-O,O-H-O,
And C-H-O type hydrogen bonds between the cationic and anionic Species help to create a delicate balance between the molecular and Super molecular charge transfer processes by creating a non-symmetry structure.

Table 1- Crystal data and structure refinement of pdn02

Chemical formula	$C_{17}H_{18}N_4O_2$	
Formula weight	310.35 g/mol	
Temperature	296(2) K	
Wavelength	0.71073 Å	
Crystal size	0.100 x 0.220 x 0.250 mm	
Crystal habit	clear light yellow Rectangular	
Crystal system	Monoclinic	
Space group	C 1 c 1	
Unit cell dimensions	a = 16.0877(10) Å	α = 90°
	b = 22.0452(13) Å	β = 93.213(4)°
	c = 17.8670(11) Å	γ = 90°
Volume	6326.7(7) $Å^3$	
Z	16	
Density (calculated)	1.303 g/cm^3	
Absorption coefficient	0.089 mm^{-1}	
F(000)	2624	

Theta range for data collection	1.57 to 25.00°
Index ranges	-19<=h<=19, -26<=k<=24, -21<=l<=21

Reflections collected	25500	
Independent reflections	9616 [R(int) = 0.0414]	
Coverage of independent reflections	99.9%	
Absorption correction	multi-scan	
Max. and min. transmission	0.9910 and 0.9780	
Refinement method	Full-matrix least-squares on F^2	
Refinement program	SHELXL-2014/7 (Sheldrick, 2014)	
Function minimized	$\Sigma w(F_o^2 - F_c^2)^2$	
Data / restraints / parameters	9616 / 2 / 841	
Goodness-of-fit on F^2	1.488	
Δ/σ_{max}	3.006	
Final R indices	3413 data; $I>2\sigma(I)$	R1 = 0.0443, wR2 = 0.0684
	all data	R1 = 0.1487, wR2 = 0.0857
Weighting scheme	$w=1/[\sigma^2(F_o^2)]$ where $P=(F_o^2+2F_c^2)/3$	
Absolute structure parameter	2.2(10)	
Largest diff. peak and hole	0.402 and -0.385 $eÅ^{-3}$	
R.M.S. deviation from mean	0.044 $eÅ^{-3}$	

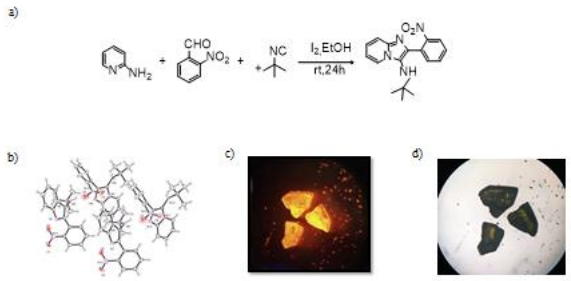

Figure 1.a) Reaction scheme, b) ORTEP view of crystal c) Crystal in Xenon lamp d) Crystal in ordinary light

FT-IR Spectral data

FT-IR (cm- ^{1})	Assignment
418.49	obo deformation
781.19	B-o-ring stretching
990.83	B-o-ring stretching

963.48 B-o-ring stretching

1149.42 Aromatic C-H inplane bending vibration.

1204.18 C-N-stretching vibration

1273.43 B-O-vibrations

1366.66 B-O-asymmetric stretching

2972.09 C-H-Asymmetric stretching vibration

3247.42 O-H symmetric stretching vibration of COOH group

FT-IR spectral data

FT-IR (cm-1)	**Assignment**
418.49	**obo deformation**
781.19	**C-Cl stretch**
990.83	**=C-H stretch**
963.48	**=C-H stretch**
1149.42	**C-N stretch**
1204.18	**C-N stretch**
1273.43	**C-N stretch**
1366.66	**C-H rock**
2972. 09	**C-H stretch**
3247.42	**N-H stretch**

FT-IR

The FT-IR spectrum is recorded in the range 400-4000cm-1 by perkin - Elmer spectrometer .FT-IR spectrum of 2pdno2 is given in figure OBO deformation is assigned to 418.49 cm-1and 781.19cm-1B-O-ring stretching,990.83cm-^{1} B-O-ring stretching1149.42cmAromaticCHinplanebendingvibratio1204.18cmstretchingvibration1273.43c1CHvibrations1366.66cm1 B-O-Asymmetricstretching,2972.09cm-1 C-H-asymmetric stretching vibration 3247.42cm-1 O- H-Symmetric stretching vibration of COOH group. The FT-IR spectrum of NBS was recorded in the range 400-4000cm-1 the frequency at which a specific group absorption is independent on its electron environment with in the molecule and its physical state.

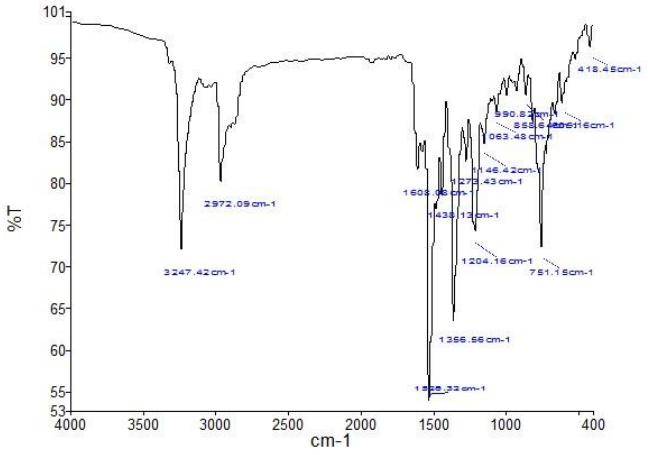

Figure 2 FT-IR Spectrum of pdn02

NMR Spectral data

$ value(ppm)	Assignment
149.49	C3 carbon of 3-nitro anilinium moiety.
142.39	C1 carbon of 3-carboxyl anilinium moiety.
132.81	C4 carbon of 3-nitro anilinium moiety.
132.38	C4 carbon of 3-nitro anilinium moiety
128.36	C6 carbon of 3-carboxyl anilinium moiety
124.35	C2 carbon of 3-nitro anilinium moiety
124.23	C2 carbon of 3-nitro anilinium moiety
123.33	C4 carbon p-toluene sulfonate moiety.
117.69	C6 carbon 0f 3-nitro anilinium moiety

111.75 C1 carbon of 3-nitro anilinium

NMR spectral studies

The carbon signal at $150ppm is attributed to the cholorin substituted . The ^{1}H NMR spectrum of pdno$_2$ crystal is shown in figure2. The intense singlet signal appearing at 2.8ppm is due the three methyl protons of p-toluene sulfonate moiety in the crystal . The C $_3$and C$_4$ aromatic protons of the same kind in the same moiety exihibit a doublet centeredat7.8ppmthecomplex multipled appearing from 8.0 to 8.2ppm is attributed to the C $_4$and c$_6$ aromatic protons in the same chemical environment in 3-carboxyl anilinium moiety . The C$_2$ aromatic proton of 3-carboxyl anilinium moiety stands responsible. for the singlet signal at 8.06ppm the multipled signal appearing from 8.6ppm to8.8ppm has been assigned to C $_5$ aromatic proton of the same moiety . The appearance of six distinct proton signals confirms the molecular structure Of the salt crystal**.** In the 1H NMR Spectrum figure Two doublets at 8.2ppm and 8.0ppm are due to to the C $_4$ and C $_6$ aromatic protons of the 2-nitrophenyl moiety respectively The triplet centered at 7.8ppm is attributed to C $_5$ aromatic proton of the 2-nitrophenyl moiety . The C4 aromatic proton of 1,2 a pyridine moiety appears as a singlet at 6.8ppm.The appearance of eleven distinct carbon signals in the 13c spectrum [fig] explicity confirms the molecular structure. In the down field two carbon signal 149.49 and 142.39ppmowe to the highly dehielded C $_1$and C $_2$carboxyl carbons of the nitrophenyl moiety. The signal at 136.19 is assigned to the C3 carbon in the same moiety .The carbon signal149.49and142.39ppm owe to the highly dehielded C $_1$and C $_2$ carboxyl carbons of the nitrophenyl moiety. The signa136.19 is assigned to the C3 carbon in the same moiety .The carbon signal 132.81ppm is due to the C $_1$ and C $_3$ carbons of the same kind in 1,2 a pyridine moiety. The signal at 128.36ppm is attributed S of the C6 carbon of the 1,2 a nitrophenyl moiety .The signal appearing at 132.38ppm is attributed to the C $_5$carbon of 1,2 a nitrophenyl moiety .The signal at 149.49,132.81,and 142.39ppm owe to the C1,C4and c2 carbons of 1,2 a nitrophenyl. moiety espectively. The carbon of 132.81ppm owes to two methyl carbon atoms .

^{1}H NMR (400 MHz, $CDCl_3$) δ 8.19 (d, *J* = 6.9 Hz, 1H), 7.91 (dd, *J* = 8.1, 1.1 Hz, 1H), 7.82 (dd, *J* = 7.7, 1.3 Hz, 1H), 7.70 – 7.61 (m, 1H), 7.59 – 7.44 (m, 2H), 7.16 (ddd, *J* = 9.0, 6.7, 1.3 Hz, 1H), 6.80 (td, *J* = 6.8, 1.1 Hz, 1H), 2.77 (s, 1H), 0.96 (s, 9H).

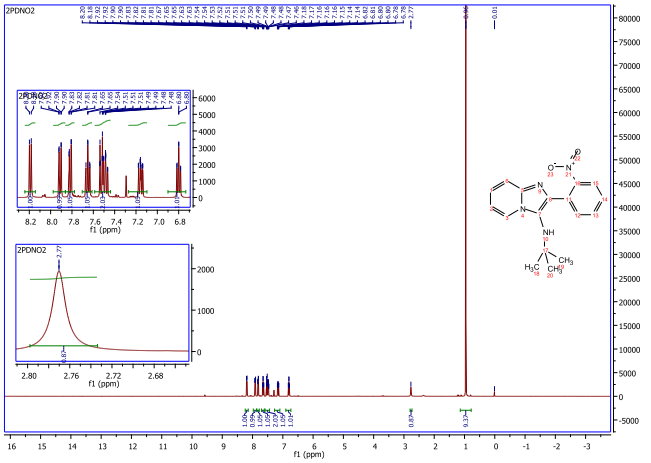

Figure 3a NMR spectrum of pdno2

^{13}C NMR (101 MHz, $CDCl_3$) δ 149.49, 142.39, 136.19, 132.81, 132.38, 128.36, 124.35, 124.23, 123.33, 117.69, 111.75, 77.40, 77.08, 76.76, 55.61, 30.04

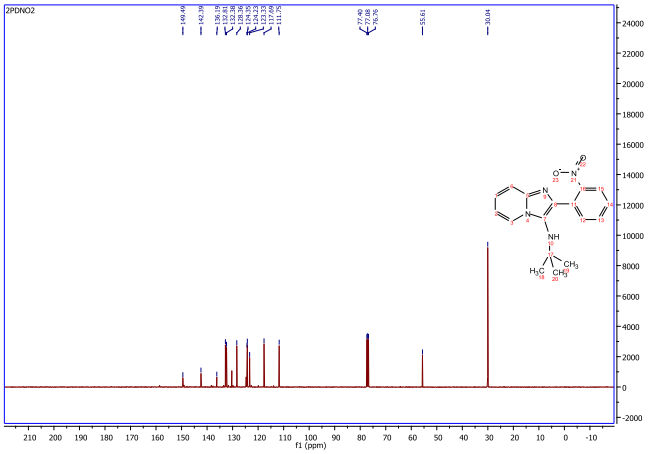

Figure 3b NMR spectrum of pdno2

Mass Spectroscopy

The lower cut-off wavelength and high optical transparency up to near infrared region are crucial parameters for an optical material. Mass spectroscopy spectrum was recorded within the range of 200-1100nm using the using lower cut-off at 300nm combined with very good transparency attest the usefulness of this material for optoelectronic applications and the generation of pdno2 .

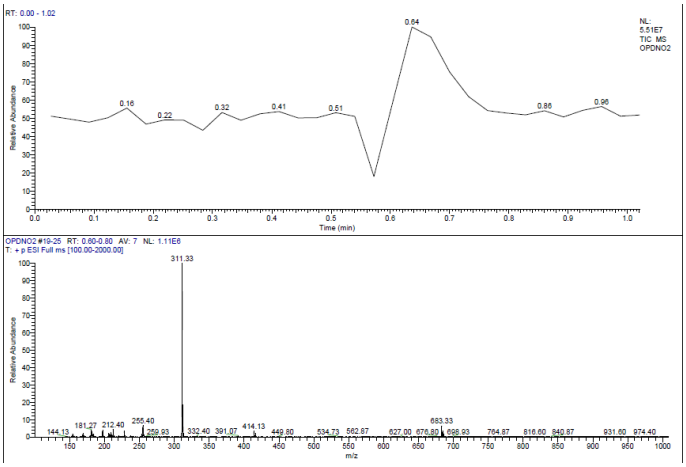

Figure 4a Mass spectroscopy of pdno2

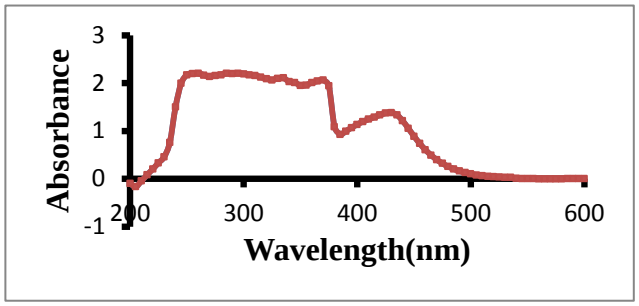

Figure 4b UV-Vis-NIR Spectrum of pdno2

UV SPECTRUM

The UV-Vis-NIR Transmission spectrum of pdno2 crystal is shown in fig.4b .The attained percentage of transmission was 45% in the visible region ,as has been observed in the spectrum there is no significant absorption in the entire visible region and near infrared region. The lower wavelength cut-off is around 400nm The crystal has a wide transparency window in the visible and NIR regions up to 2500nm. This wide transparency window enables the title crystal to be a potential candidate for the optical applications. The absorbance 305and1 100nm is illustrated. above 200nm and absorbance due to electronic transition between 305 to 1100nm.This less absorbance in the entire visible and near-IR region is an important requirement for NLO applications. The UV –Vis –NIR Spectral study was carried out using a T 90+PG instruments spectrophotometer A optically transparent crystal with 1.2 mm thickness was used for this study The pdno2 crystal has sufficient transmittance in the entire visible ,near UV and IR regions and has good transparency about 60% (fig.4b).The power cut-off wavelength of pdno2 of was found to be 231nm and the absorption is due to the promotion of an electron from a 'non-bonding' (lone-pair) n-orbital to an 'anti-bonding' #-orbital designed as #* (n _#*).The absorption coefficient (a)was estimated from the transmission spectrum based on the following relation.435 nm and 295 nm EtOH solvent used 10uM concentration sample per mL

TGA

Thermo gravimetric Analysis

Thermal studies

Thermal analysis was performed on the grown crystal to study the thermal stability and melting point. The thermo gravimetric analysis of LHFFA was carried out between room temperature (28 ° c)and 1200 °c heating rate 20° c/min in nitrogen atmosphere using SDT Q6000 V8.2 Built 100 thermal analyser. The TGA And measurements show the mass variation recorded during the heating . The results are shown in figure .The obtained TGA curve shows sudden weight loss at 221.47° c A powered sample weighing 24 mg was used for the analyses . The analyses were carried out simultaneously in air at a range of 1-100c and are represented in fig. the thermo gravimetric analysis shows that the sample has good thermal stability up to 180°c . The absence of water of crystallization in the molecular structure is indicated the absence of weight loss around 100°c and .Further there is no decomposition up to up to the melting point. The material decomposes at 221.47°c which is represented by the structure of loss of the mass. Above 221.47°c the material undergoes irresverable endothermic transition at 309.42°c The thermo gravimatric (tg) were carried out in a nitrogen atmosphere from temperature to 773k.The decomposition occurs in two stages .The first stage incurred weight loss 17.22% at 309.42°C and the second stage of 94.95 %. The sharp exothermic peak 221.47°C corresponds to the melting point of the substance The absence of water of crystallization in the molecular structure is indicated by the absence of weight loss around 100c further there is no decomposition up to the melting point. The material decomposes at 228. 29c which represented by the students of loss of the mass. above 228.29 c the material undergoes irrversible endothermic trasition at 338.99.The differential scanning calorimeter (dsc) is carried out using SDT Q290 v23.10 build 79 analyzer between 50 and 300c in the nitrogen atmosphere at a heating rate of 50 c/min and its shown in figure. In the

DSC the endothermic peak observed near 300c corresponds to melting and the deuteration content of the synthesized material prior to the growth of DGPI was examined though differential scanning calorimeter (dsc) analysis . The sharp endothermic peak at 276.67 c (figure) reveals that the starting material was not fully deuterated after the completed of the growth ,the dielectric measurements were carried out in order to understand the phase trasition temperature which is the direct evidence of the in corporation of the deutration regions of negative v(r)are usually associated with the long pair of electro negative atoms .As can be seen from the MEP map of the title crystal which regions having the negative potential are over the electro `negative at(nitrogen and oxygen atoms)the regions having the positive potential are over the hydrogen atoms from this result. we can say that the H atom a indicate the strongest attraction and o atom indicate the strongest repulsion.

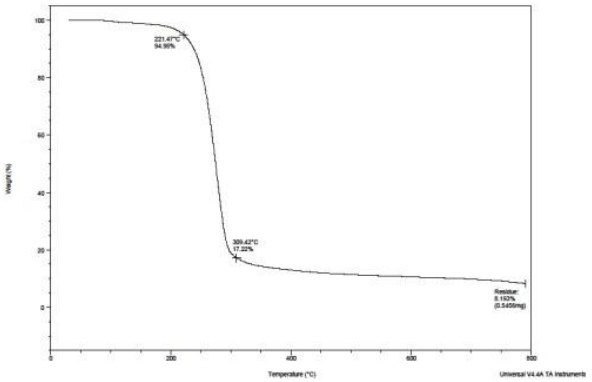

Figure 5 Thermo gravimetric analysis curve of pdno2

SECOND HARMONIC GENERATION

The output from Q-switched Nd: YAG laser (λ=1064nm) model GCR-2 (10) Was focused on the powered GOX sample .Pulse energy was 5MJ/S with pulse width of about 10ns. A bright green flash emission from the GOX sample was observed which indicates the NLO behaviour of the material .The second harmonic generation efficiency of Gox was compared with $pdno_2$ .The SHG output of $pdno_2$ was 240mv and Gox had 210mv at given pulse energy of 5MJ/S. The SHG property of $pdn0_2$ is determined by the midified version of powder technique by Kurtz and perry. The fundamental beam of λ=1064nm from Q-switched Nd: YAG laser is used to test the SHG property of the grown crystals. The input pulse energy 1.6MJ/pulse is used $pdn0_2$[150nm] is used as the reference material SHG of $pdno_2$ is measured as 135 mv which is 0.9 times that of $pdno_2$.The SHG behaviour of the title crystal was confirmed from the green light emission.

Third order nonlinear optical properties

The third order nonlinear refractive index and the nonlinear absorption coefficient were evaluated by the z scan measurements. In this method the sample is translated in z direction along the axis of a focused gaussian beam from the He-Ne laser at λ = 632.8nm and the far field intensity is measured as a function of the sample position. It allows the simultaneous measurements of both the nonlinear refractive index and the nonlinear absorption coefficient .non-linear refractive index n_2 was calculated by the relation

. $n_2 = \frac{\Delta\emptyset}{KI_o left}$

where k is wave vector, Io is intensity of the laser beam at focus (z=0) left is affective thickness of the material and ^Ø is phase shift.

The nonlinear absorption coefficient was estimated from the open aperture z-scan data using the relation.

$$\beta = \frac{2\sqrt{2}\Delta T}{Io\ left}$$

where ▲T is one valley value at open aperture z-scan curve .The read and imaginary parts of the third order nonlinear susceptibility are defined as,

$$Re\ X^{(3)} = \frac{10^{-4}}{\epsilon o\ c^2\ no^2 \Delta\emptyset}$$

$$\pi$$

$$I_m\ (x)^3 = \frac{10^{-2}}{\epsilon o\ c^2\ no^2\ \beta}$$

$$-4\pi^2$$

where ϵo is premitivity of the vacuum ,no is linear refractive index of the material and c is velocity of light $X^{(3)} = \sqrt{[Re(X^{(3)})]^2 + [lm\ (x^{(3)})]^2}$ closed aperture and open aperture z-scan curves are given in fig. from the closed aperture z-scan measurements ,the nonlinear refractive index was calculated as $0.760335*10^{-9}$ cm^2/W. The positive value of nonlinear refractive index shows that the crystal has a self-focusing nature, open aperture z-scan measurements concluded that the nonlinear absorption co-efficient of the mat erial is $-0.06311257*10^{-4}$ Cm/W .The third order nonlinear susceptibility $x^{(3)}$ was calculated as $1.259459*10^{-3}$ esu. The calculated third order non-linear optical values of pdno2.

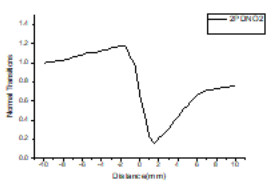

Figure 5a : Z- scan of closed curve

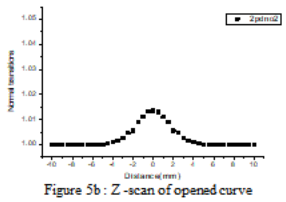

Figure 5b : Z -scan of opened curve

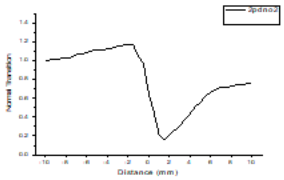

Figure 5c : Z-scan of Ratio curve

Figure 6 Z-scan Third order nonlinear optical properties

THIRD ORDER NON-LINEAR OPTICAL VALUES OF $PDNO_2$

Non-linear Refractive index non-linear absorption coefficient (cm

n2 (cm2/w) $8.041*10^{-8}$ /w) 0.015*10-4

Real part of susceptibility Re Imaginary part of susceptibility Im

X(3) (esu)2.107*10-6 X(3) (esu) 0.094*10-6

Third order susceptibility X(3) (esu)1.017*10-3

x3 values of some NLO crystals

crystal
x(3) (esu)

$Pdno_2$
2.109*10-4

He-Ne laser (5mw) source of wavelength (λ =632.8nm) with the beam diameter of 0.5mm was used for the Z-scan experiment . The gaussian input laser beam generated by focusing via Gaussian filter was projected through a convex lens placed at a focal length of 30mm in transverse mode operation . High power laser damage tolerance factor decides the performance of an optical material to be employed in laser power related device applications.

z-scan

He-Ne laser (5mw) source of wavelength (λ =632.8nm) with the beam diameter of0.5 mm was used for the Z-Scan experiment the Gaussian input laser beam generated by focusing gausssian filter was projected through a convex lens placed at focal length of 30mm in transverse mode operation High power laser damage tolerance factor decides the performance of an optical material to be employed in laser power related device applications .LDT measurements was performed on (020)facet of grown BCFF crystal using laser (λ =1064mm)source .The laser beam of1mm diameter and pulse width of 10ns with the frequency rate of 10HZ was used in this experiment .The damage occurred of the surface of the crystal placed at a focal length of 30cm due to laser irradiation and its energy density was measured using a power meter (model NO:EPM 2000) . The LDT value can be calculated using the expression.

Differential Scanning Calorimeter

The differential scanning calorimeter (dsc) is carried out using SDT Q290 v23.10 build 79 analyzer between 50 and 300°c in the nitrogen atmosphere at a heating rate of 50 °c/min and its shown in figure 6 .in the DSC the endothermic peak observed near 300°c corresponds to melting and the deuteration
content of the synthesized material prior to the growth of DGPI was examined though differential scanning calorimeter (dsc)analysis . The sharp endothermic peak at 276.67 °c (figure) reveals that the starting material was not fully deuterated after the completed of the growth ,the dielectric
measurements were carried out in order to understand the phase trasition temperature which is the direct evidence of the in corporation of the deutration regions of negative v(r)are usually associated with the lone pair of electro negative atoms .As can be seen from the MEP map of the title crystal which regions having the negative potential are over the electro`negative atoms (nitrogen and oxygen atoms)the regions having the positive potential are over the hydrogen atoms from this result. we can say that the H atom a indicate the strongest attraction and o atoms indicate the strongest repulsion.

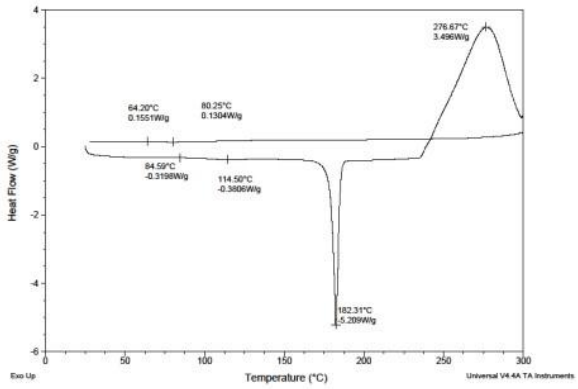

Figure 7 differential scanning calorimeter curve pdno2

III. RAMAN SPECTROSCOPY:

Raman spectrum of $pdno_2$ crystal are recorded using BRUCKER RFS 27 FT-Raman spectrometer with Nd:YAG, laser (λ=1o64 nm) sample was scanned over the range of 500-400cm-1 . The recorded FT-Raman spectrum is shown in figure peak observed for a given energy of the laser beam, the strength of Raman scattering depends on (frequency) and it was for this reason that lasers in the high-frequency, visible end of the spectrum were formely used. more recently, however ,near-infra-red laser excitation has been successful, usually using NdYAG laser operating at 9398cm-1 .An added economy is that ,once the optical path of the FT spectrometer has been properly aligned, it is a fairly simple matter to interchange sources, beam slitters and detectors, and a single FT instrument can thus be operated either as an infra-red spectrometer or as A Raman spectroscopy In this section we shall discuss some examples of the combined use of Raman and infra-red spectroscopy to determine the shape of some simple molecules be limited and the molecules considered (CO2,N2o,Clf3)have been chosen to illustrate the principles used; extension to other molecular types should be obvious. details first with the triatomic AB2 molecules types should be decided are whether each molecule is linear or not and ,if linear, whether it is symmetrical (B-A-B) or asymmetrical (B-B-A). in the case of carbon dioxide and nitrous oxide ,both molecules give rise to some infra-red bands with PR contours; they must, therefore, be linear. The mutual exclusion rule shows that C02 has a center of symmetry (O-C-0)while N2Ohas not(N-N-O),since only the latter has bands common to both its infra-red and Raman spectra, Thus the structures of these molecules are completely determined. When a beam of light is passed through a transparent substance ,a small amount of the radiation energy is scattered, the scattering persisting even if all dust particles or other extraneous matter are rigorously excluded from the substance. If monochromatic radiation ,or radiation of a very narrow frequency band, is used ,the scattered energy will consist almost entirely of radiation of the incident frequency (the so-called Rayleigh scattering)but, in addition, certain discrete frequencies above and below that of the incident beam will be scattered ;it is this which is referred to as Raman scattering. The symmetric modes of vibration are parallel and Raman polarized.

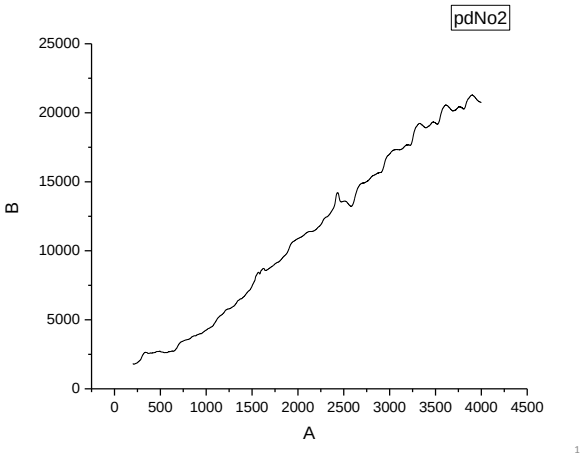

Figure 8 Raman spectroscopy of crystal $pdno_2$

IV. CONCLUSION

The molecular structure was established by single crystal XRD analysis and further confirmed by NMR spectroscopic study. The presence of various functional groups in the title salt has been confirmed by FT-IR spectrometer Study. These crystals were subjected into various characterizations. single crystal XRD analysis shows that pdno2 crystal belong to triclinic crystal system with lattice parameters a=16.08779(10) A, b=22.0452(13)A,C=17.8670(11)A. Single crystal X-ray studies confirmed the cell parameters of pdn02 crystal. which can be employed in the NLO `Applications in the entire visible region. In mass spectroscopy spectral analysis ,the cut off wavelength was found to be 456nm. and the near IR region. UV -Vis The studies shows that it has a wide range of transparency region(second order NLO studies show that the pdn02 crystals can be used for the nonlinear properties .The relative SHG efficiency of pyridin-3-amine was found to be 1.34 times that of standard pdno2 crystal. The functional groups are assigned using FT-IR and FT-Raman spectroscopy. The UV-Visible spectrum reveals that the grown Thermo have the gravimetric and differential thermal analysis shows that the crystal is stable up to 200c. The order nonlinear optical properties are calculated using Z

scan technique . Deuteration content of the as grown crystals perfection analysis reveals that the quality of the

grown was good without any internal structural boundaries. The recorded FT-IR spectrum confirms the presence of various functional groups as well as existence of inter-molecular hydrogen bonding between the constituent species. The thermal behaviour of the grown crystal was studied by TGA-DSC analyses. The single and multiple shorts laser damage threshold values and the relative SHG efficiency of pzn02 were found out.

REFERENCES

[1]k. sangwal. J. crystal Growth 97 (1989) 393
[2]I.OWCZAREK, k. sangwal. J. crystal Growth102 (1990) 574
[3]L.N. Rashkovich, KDP Family of single crystal, Adam Hilger, New York ,1991
[4]J.W.Mullin, crystallization, thirded, Butterworth Hinemann London,1993
[5]Atlomare.A. cascarano. G. Giacova ZZo.c.Guagliardi,A.Burla.M.c.polidori,G&Gamali.M(1994)Appl. cryst.27.435
[6]J.Yabuzaki.T.Takahasmi H.Adiuchi Y.Mori, T.sasaki Bull.Mater.science 22 (1999)11-13
[7]G.A. Jeffery. An Introduction to Hydrogen Bonding oxford university press, New York-1997
[8]J.B. Gaudry L. caps. p. Langot s.Marcen, M.kollmannsbergerO.Lavastrte,E.freysh,J.F.Letard,o.skahn,chem. phys.Lett.324 (2000) 321-329
[9]L.M.Epstein,E.s.shubinacoord.chem.Rev,23 (2002) 165-181s
[10]M.Makowska-Janusika, E.Gondek.I.V.kityk, J.wisla J.sanetra,A.danel,chem..phys.306s (2004) 265-271
[11]Tanusripal.Tanusree kar,Gabriele Bocelli,Lara Rigi,cryst.Growth.Des.3(2003)13
[12]A.datta,s.k.pati,chem..Eur J.11(2005) 4961
[13]L.R.Dalton,P.A.sullivan,B.C.olbricht.D.H.Bale B.C.Olbricht.D.H.Bale J.Takayesh,s.Hammond H.R0mmel,B.H.Robinson,Tutorials in complex photonic smedia,SPIE,Belingham,WA,2007
[14]. V.krishnakumar,s.kalyaranama,M.piasecki,I.V.KITYK,P.Bragid J.Raman spectrosc,39 (2008)1450-1454.
[15].Ramachandra Raja,A,Antony.Josesh:Mater.Lett.63 (2009) 2507-2509s
[16]Gana sambandam c.perumal s.J.Cryst Growth 2010 :312:1599
[17]Nagalakshmi R.krishnakumar V.Hagemann.H.Muthunatesan s.J.Mol structure.2007 832:101
[18]peramiyan G.pandi p.sorna murthy BM.Mohan kumar R.Adv.matter Ros 2012:584:13
[19]k.Boopathi,p.Rajesh,p.Ramasamy.p.Manyum.opt.Mater.35 (2013)954
[20]A.Arunkumar.p.Ramasamy.Mater.Letter.123 (2014) 246-249
[21]S.karthiga. kalainatahn k. Umameshwara SRao,F.Hamada.M.Yamada.y.kondo.J. cryst. Growth 436 (2016) 11 3-124
[22] R. Dhanjayan N.sivakumar s.Gunasekar s.srinivasan J.Matter.196 (2017) 74-77

